

## 1 1. Introduction

2  
3 Numerous studies have addressed the issue of the urban heat island (UHI) in different  
4 regions of the world, especially where urban areas have replaced natural vegetated surfaces in  
5 temperate and subtropical environments. The results of these studies have indicated that urban  
6 areas show higher land surface and/or air temperatures than surrounding rural areas, particularly  
7 at night-time (e.g. Coseo and Larsen, 2014; Hu and Brunzell, 2013; Zhang et al., 2013).  
8 However, in hot arid environments, where urban areas are replacing desert sands, urban heat  
9 sinks (UHS) can be detected, where urban land surface temperature (LST) is lower during the  
10 daytime than the surrounding desert (Frey et al., 2007; Imhoff et al., 2010; Lazzarini et al.,  
11 2013).

12 The magnitude of the observed UHS in desert regions can depend on many factors  
13 including weather conditions and the timing of temperature observations, but it has been  
14 suggested that the characteristics of the urban land cover exert a major control on variations in  
15 land surface temperature (Carnahan and Larson, 1990). The UHS effect has been attributed to an  
16 increase in vegetated areas associated with urbanization which generate a cooling effect due to  
17 the increase in latent heat flux through evapotranspiration and a decrease in sensible heat relative  
18 to the desert surroundings (Lazzarini et al., 2013). However, other studies have shown that desert  
19 cities can still exhibit an UHS despite containing little vegetation and being primarily composed  
20 of impervious surfaces (Frey et al., 2007; Imhoff et al., 2010), although no evidence was  
21 provided to explain these findings. This disparity in the literature highlights the need for further  
22 research to understand the relationships between land cover and LST in desert cities.

23 The properties of the urban fabric can also influence the UHS; it has been suggested that  
24 highly reflective materials, or those with a low thermal conductivity, can contribute to urban

1 cooling (Erell et al., 2011; US EPA, 2008). Some cities have made use of highly reflective  
2 materials on rooftops, roads and parking lots to increase albedo hence reduce the absorption of  
3 solar radiation and surface temperatures (Bretz et al., 1998). For example, Mackey et al. (2012)  
4 found that increasing the surface reflectivity in urban areas of Chicago had a stronger cooling  
5 effect than increasing the amount of vegetation cover. Similarly, increasing the specific heat  
6 capacity of urban materials has been shown to decrease daytime summer peak temperatures by  
7 postponing the release of stored heat (Hamdi and Schayes, 2009), although this is likely to  
8 contribute to an urban heating effect at nighttime. Moreover, urban water bodies can make a  
9 significant contribution to cooling due to their high specific heat capacity and ability to lose heat  
10 via evaporation (Omran, 2012). However, the overall contribution of variations in the thermal  
11 properties of different surface materials has received little attention in the context of the UHS  
12 phenomenon in desert cities.

13 Evidence concerning the impact of urban geometry on thermal conditions is somewhat  
14 unclear. Several studies have demonstrated that an increase in building height and density  
15 produces an increase in surface temperature (e.g. Martin et al., 2012; Wu et al., 2013).  
16 Conversely, other research suggests that tall buildings and narrow streets generate shadow  
17 effects which decrease the absorption of solar energy at the land surface thus lowering  
18 temperatures (e.g. Littlefair et al., 2000; Kato et al., 2010). There is also evidence that variability  
19 in building height is important, with areas containing a diverse range of building heights  
20 generating an increase in wind speeds and natural ventilation at street level leading to a decrease  
21 in surface temperature (Johansson and Emmanuel, 2006). Given that these cooling mechanisms  
22 have been recognized, it is now important to determine the relative contribution of urban  
23 geometry to the overall UHS effect in desert cities.

1           Although the UHS effect in desert regions has been identified there is considerable  
2 uncertainty over the factors which generate this phenomenon. Hence, the aim of this study was to  
3 improve our understanding of the causes of cooling in desert cities. The study site was Dubai,  
4 United Arab Emirates (UAE), which has experienced rapid urbanization over the last 25 years.  
5 We used data from the Landsat image archive to address the following research objectives: (i) to  
6 characterize changes in land cover, land use and albedo that have taken place as a result of  
7 urbanization; (ii) to quantify the development of the UHS during urbanization; (iii) to examine  
8 whether variability in the magnitude of the cooling effect can be explained by the transitions in  
9 land cover, albedo and type of land use; and (iv) to evaluate the sensitivity of the UHS to  
10 variations in urban geometry.

## 11 **2. Study area**

12  
13           Dubai Emirate (Figure 1) is one of the fastest growing cities in the Middle East. The total  
14 area of the emirate is approximately 3885 km<sup>2</sup> and it is characterized as a hyper arid environment  
15 with an annual average rainfall of only 8mm falling mostly in the late autumn and winter months  
16 (Dubai Airport, 2014). The warmest months in Dubai are May to September with an average  
17 maximum temperature of 40°C and average minimum of 28°C; the coldest months are December  
18 to February with an average maximum temperature of 25°C and average minimum of 15°C

19           After the discovery of oil in the late 1960s, Dubai attracted a large overseas labour force.  
20 Consequently, the population increased from 183,187 in 1975 (National Bureau of Statistics,  
21 2010) to 2,003,790 inhabitants in 2011 (Dubai Statistical Centre, 2011). The physical size of the  
22 urban area has grown dramatically over time as the desert has been transformed into residential,  
23 commercial, sports and tourism developments. This growth was a consequence of the strategic  
24 plan of the Emirate to diversify the economy by stimulating real estate marketing and developing

1 tourism attractions. Indeed, the rapid pace of desert alteration in Dubai has attracted the attention  
2 of economists, environmentalists and urban planners.

3         According to the Skyscraper Center (2014), 180 buildings in Dubai are greater than 100m  
4 in height in 2011, while there are also many other areas of low-rise urban development, making  
5 Dubai an excellent study site to investigate the effect of urban geometry on the UHS in desert  
6 cities. Furthermore, due to the strong and systematic urban planning process in Dubai, large  
7 discrete blocks of different urban land use types have been created, making this a useful study  
8 site for investigating the impact of land use on the cooling effect. The recently developed  
9 offshore islands (see Nassar et al., 2014) were not included in the study area but the  
10 environmental impacts of the islands are being investigated in our ongoing work.

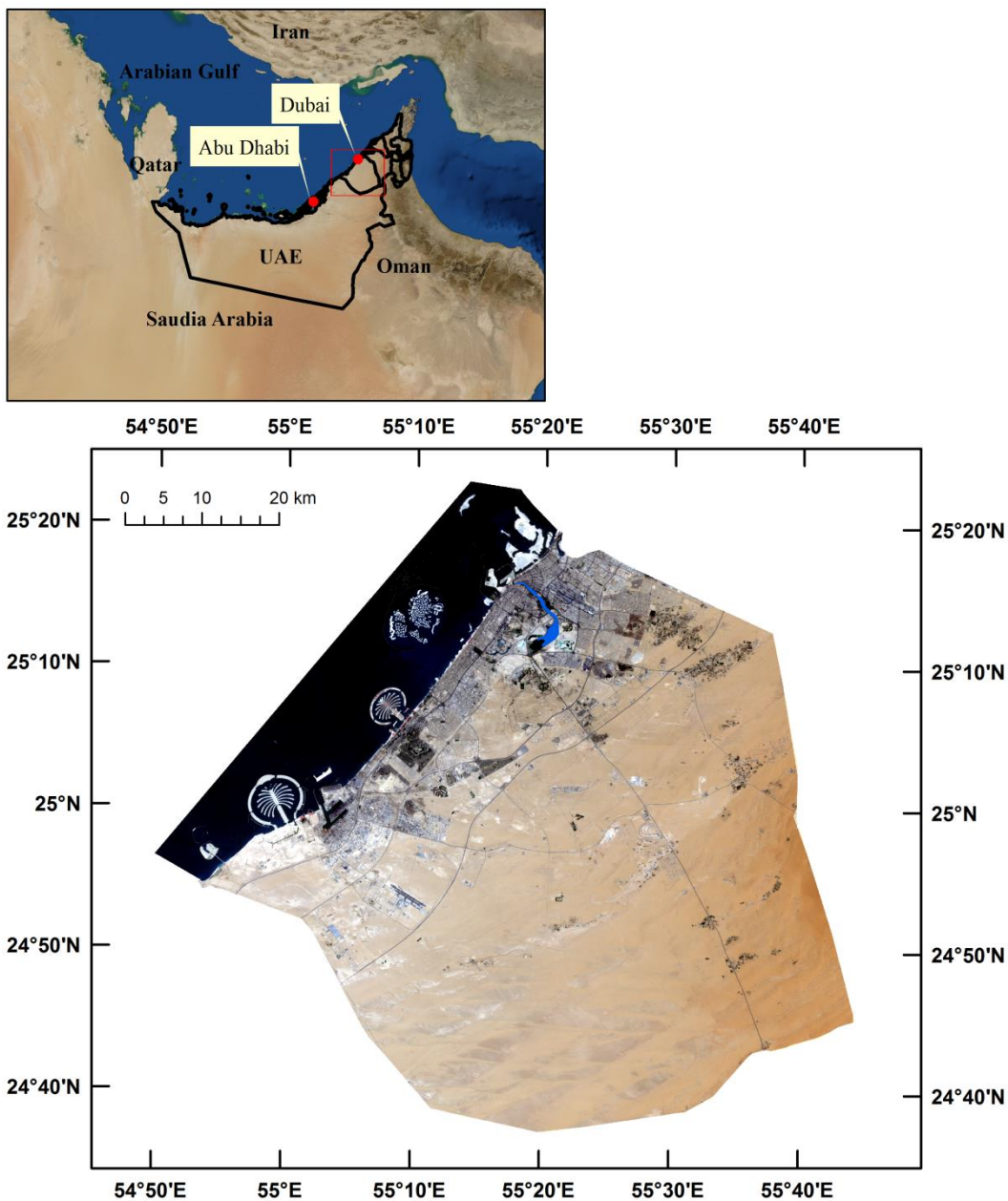
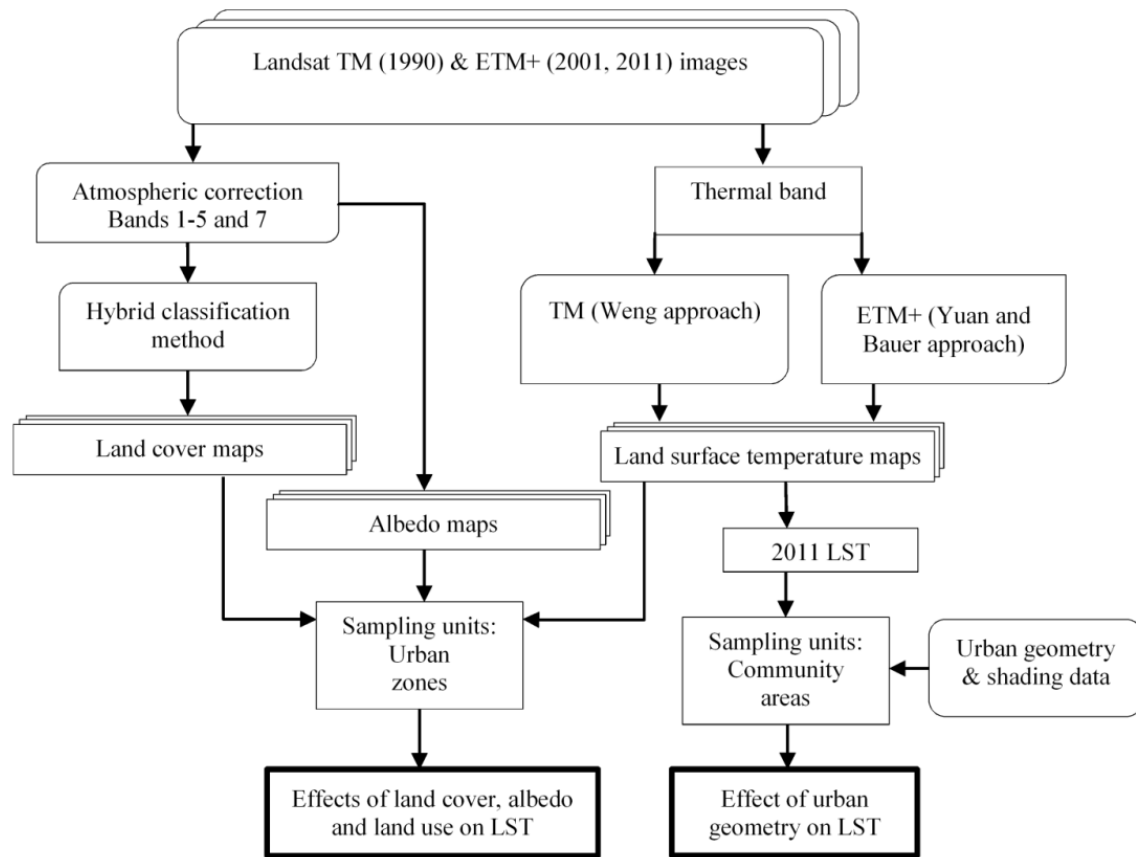


**Figure 1.** Overview map of the Arabian Gulf and map of the study area, Dubai Emirate, United Arab Emirates (UAE) based on a Landsat ETM+ scene from 2011(RGB-321).

### 1 3. Materials and Methods

2 Figure 2 shows the main stages of data processing and details are provided in the following subsections.



1

2 **Figure 2.** Flowchart showing the main stages of data processing and analysis.

3 **3.1 Data acquisition and image pre-processing**

4

5 Three Landsat scenes, acquired in August 1990, 2001 and 2011 (Table 1) were used to capture  
 6 the main period of rapid urbanization in Dubai. Previously, the largest UHS effects have been  
 7 observed during the daytime in the summer (e.g. Imhoff et al., 2010; Lazzarini et al., 2013)  
 8 hence the Landsat scenes chosen for this study were the most appropriate for examining the  
 9 variability of the UHS in Dubai over space and time. All the images were cloud free, which  
 10 greatly helped in the land cover (LC) classification and retrieval of LST and albedo. All images  
 11 were acquired as close as possible to the same Julian day in order to minimize the effects of  
 12 variations in solar geometry.

**Table 1**

Satellite images used in the study.

Date YY-MM-DD	Local time overpass	Satellite number (sensor)	Sun elevation (degrees)	Sun Azimuth (degrees)	Spatial resolution of bands
90-08-28	10:14:55	Landsat4 (TM)	56.631	110.737	TIR: 120m; other bands:30m
01-08-26	10:35:19	Landsat7 (ETM+)	61.116	114.745	TIR: 60m; other bands:30m
11-08-22	10:39:57	Landsat7 (ETM+)	62.678	113.0399	TIR: 60m; other bands:30m

1

2 Atmospheric correction for bands 1-5 and 7 was conducted using the Fast Line of Sight

3 Atmospheric Analysis of Spectral Hypercubes module within ENVI and the original digital

4 numbers were converted to surface reflectance (Kayadibi, 2011). The images were then co-

5 registered with existing map data on a WGS 84 datum/Dubai Local Transverse Mercator

6 projection using 57 ground control points which were distributed around the images to maximize

7 registration accuracy (Jensen, 2005).

### 8 **3.2 Land Cover (LC) classification and derivation of Land Surface Temperature (LST) and** 9 **albedo.**

10

11 A hybrid classification method was applied to the atmospherically corrected Landsat

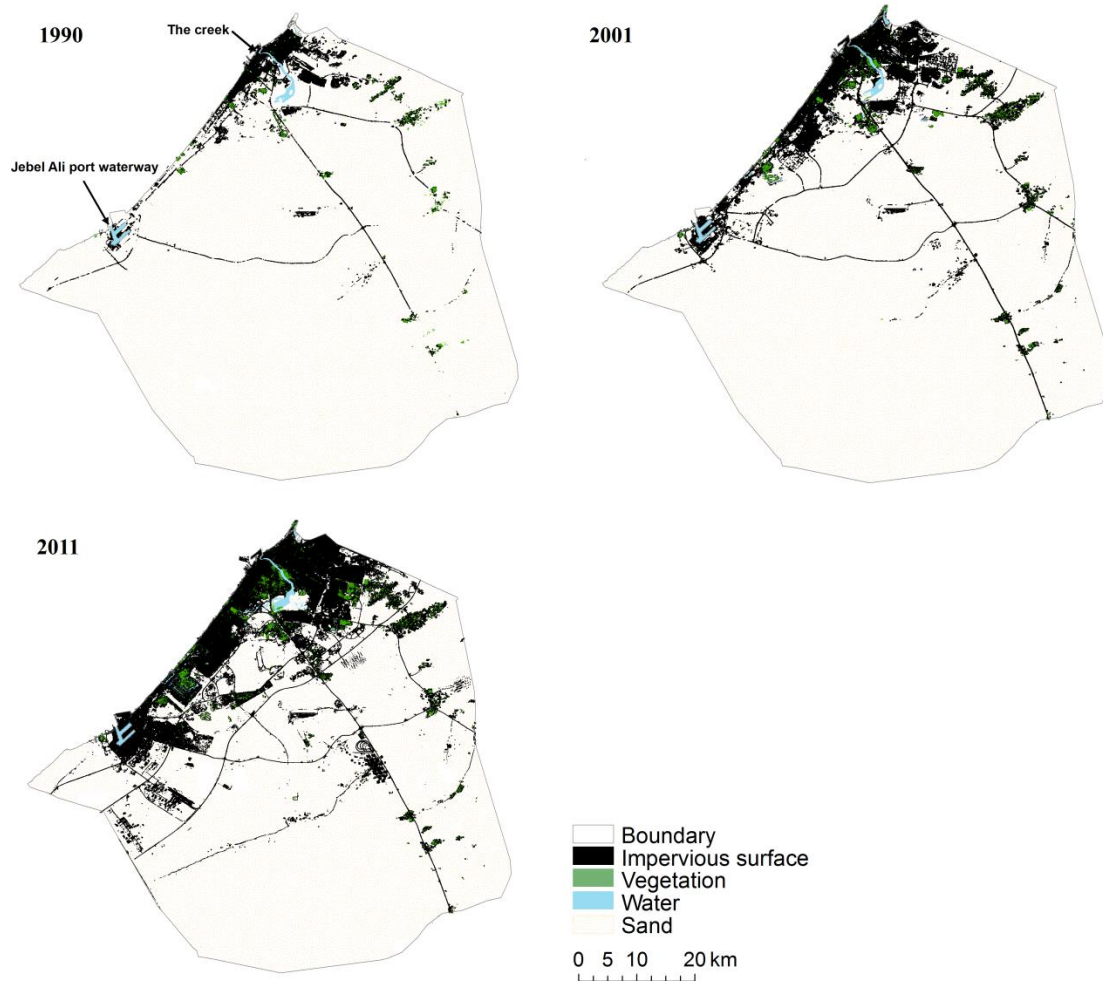
12 images to derive LC maps for the three sample years (Figure 3). This hybrid method of

13 classification is based on a combination of unsupervised and supervised algorithms and exploits

14 the advantages of both approaches to overcome their limitations (Lo and Choi, 2004). This

15 method has previously proven effective for discriminating urban areas in desert environments

16 (Nassar et al., 2014).



1

2 **Figure 3.** Land cover characteristics in Dubai in 1990, 2001 and 2011. The specific locations in  
 3 the 1990 map are labelled because they are referred to later in the text.

4

5 To assess the accuracy of the classified images, 60 stratified random samples (image and  
 6 reference pairs) were collected for each class and these samples were independent from the data  
 7 used for training to avoid bias (Verbyla and Hammond, 1995). The reference sample classes  
 8 were identified through manual interpretation of high resolution imagery from Dubai Sat-1 (for  
 9 2011), IKONOS (for 2001) and aerial photography (for 1990). The overall accuracies for the  
 10 three classified images ranged from 89-93% which exceeded the minimum 85% accuracy  
 11 recommended by Anderson et al. (1976).

1 LST was obtained from the single thermal channel of Landsat TM/ETM+ using the  
 2 methods of Weng (2001) for Landsat TM and Yuan and Bauer (2007) for Landsat ETM+. In  
 3 both methods the emissivity effects were corrected using an approach developed by Snyder et al.  
 4 (1998). LST values derived from both the TM and ETM+ data were subsequently converted  
 5 from Kelvin to degrees Celsius by subtracting 273.15. Surface albedo was retrieved by using the  
 6 atmospherically corrected reflectance values from TM and ETM+ based on the approach of  
 7 Liang (2000).

8 **3.3 Land use (LU) map and sampling of Land Surface Temperature (LST), albedo and Land**  
 9 **Cover (LC).**

10  
 11 A LU map for the urban area of Dubai (as of 2011) was constructed by manually  
 12 digitizing the boundaries of zones of different LU types by incorporating information from the  
 13 Landsat-derived LC map for 2011, existing land use maps and through visual interpretation of  
 14 high resolution images on Google Earth<sup>TM</sup>. Five urban LU types (Table 2) were mapped in this  
 15 way resulting in 55 different urban zones with a total area of 859km<sup>2</sup> (Figure 4).

16  
**Table 2**  
 Land use classification schema employed in this study.

LU type	Description
Residential	All types of distinctive residential communities.
Mixed	Both residential and commercial that cannot be separated.
Recreational	Parks, golf courses and playgrounds.
Industrial	All types of light and heavy industrial plants.
Transportation	Airports and seaports.

17  
 18 Six sample areas covering the desert were also digitized (Figure 4) and used as reference sites to  
 19 represent the original natural land cover surface in the study area. The boundaries of the urban  
 20 zones and the desert samples were then used as spatial sampling units to extract data from the

1 LST maps from 2011, 2001 and 1990. The mean LST was calculated for each zone (i.e. all LST  
2 pixels falling within each polygon were averaged) and for the whole area covered by the desert  
3 samples. For each of the sampling years, the difference in LST between each urban zone and the  
4 desert was calculated in order to express the LST of each urban zone relative to the desert ( $LST_r$ )  
5 for each year. This avoided the use of absolute LST measurements which can vary between  
6 sampling years according to meteorological conditions leading up to and at the time of  
7 acquisition of each of the Landsat scenes. Furthermore, the use of  $LST_r$  measurements accounted  
8 for any residual effects of atmospheric interactions or differences in sensor types between  
9 Landsat image acquisitions which may have still been present in absolute LST measurements  
10 despite the extensive preprocessing effort. Hence, the use of  $LST_r$  data for each of the three  
11 sample years allowed us to quantify the changes over time in the magnitude of the UHS effect  
12 for each urban zone.

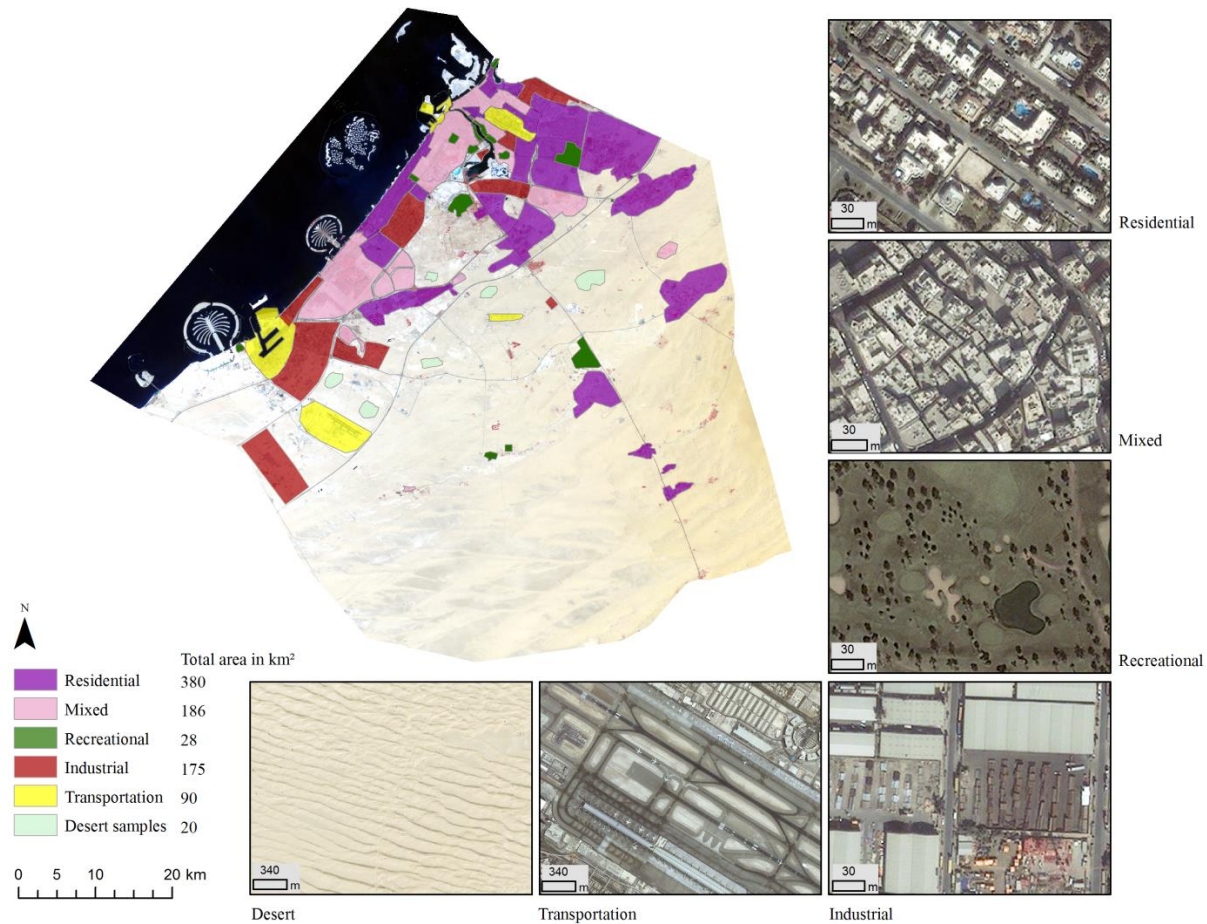


**Figure 4.** Map of urban zones in Dubai in 2011. Each zone is represented by an individual polygon (55 in total) and the colour of the polygon represents the land use type within each zone. The areas used to sample desert land surface temperature are also shown. The Landsat ETM+ scene from 2011(RGB-321) is displayed in the background. Example images from IKONOS of the five urban land use types and the desert are inset.

1           The boundaries of the urban zones in 2011 were then used to extract data from the LC  
 2 and albedo maps from 2011, 2001 and 1990. For each urban zone the areal percentage of each  
 3 anthropogenic cover (impervious surface, vegetation and water) and the average albedo was  
 4 calculated for each year. Generating the datasets in this way meant that we were able to sample  
 5 across urban zones that have undergone a wide range of different types of transitions, from the  
 6 extremes of zones which were urban in 2011 but entirely desert in 1990, through to zones which  
 7 were urban in 2011 and had essentially remained so from 1990; the data sampled across all of the

1 different LU types and incorporated a wide variation in the composition of LC. These data sets  
2 were subsequently used to assess (graphically and statistically) how changes in LU type, LC  
3 composition and albedo in the urban zones have influenced  $LST_r$  over time.

#### 4 ***3.4 Urban geometry variables and associated LST***

5 Information on urban geometry was derived from a vector layer of building ‘footprints’  
6 and associated height attributes (source: Dubai Municipality). These data were only available for  
7 2011 hence we restricted our analysis of the impacts of urban geometry on LST to this year. This  
8 was a large and spatially-precise dataset but only covered a proportion of the entire emirate  
9 (73km<sup>2</sup>) hence it was inappropriate to use the (large) urban zones as the sampling units (as in  
10 section 3.3) for the analysis of urban geometry effects. Instead, we used the boundaries of  
11 ‘communities’ as the sampling units; these are defined administrative areas in Dubai, within  
12 which, due to the systematic planning process, the form of urban development is consistent. The  
13 spatial extent of the buildings layer coincided with 116 community boundaries and incorporated  
14 a variety of different urban forms ranging from areas dominated by high rise construction with  
15 wide streets through to low-rise, high density buildings with narrow streets. The buildings  
16 dataset was used to derive average building height, variability in building height (standard  
17 deviation) and building density for each community. The 3D Analyst extension in ArcGIS was  
18 then used to simulate the area of shadow cast by the individual buildings, based on the actual  
19 solar azimuth and zenith angles at the time of acquisition of the 2011 Landsat ETM+ image. The  
20 areal percentage of shade per community was then summarized. The community boundaries  
21 were also used to summarize the average LST per community from the 2011 LST image. Hence,  
22 these data sets enabled analysis of the influence of building height, density and shadow on LST.

1 **4. Results**

2 ***4.1 LC and LU change in Dubai***

3

4

5         Some context for the subsequent results is provided by the LC and LU changes that have  
6 taken place during the urbanization of Dubai. From 1990 to 2011, the area of impervious surface  
7 increased by 423km<sup>2</sup> with a compound annual growth rate of 7.5%, while vegetated areas  
8 increased by 25km<sup>2</sup> with an annual growth of 4.9%. Inland water (excluding the Creek and Jebel  
9 Ali port waterway) increased from 0 to 2km<sup>2</sup> but this cover type still only occupied 0.2% of the  
10 total area of Dubai in 2011. All of these changes in LC occurred at the expense of desert sand.  
11 Changes in LC that have taken place within each of the different LU types are summarized in  
12 Table 3. By 2011 there was considerable variability in the percentage of impervious surface  
13 coverage across the different LU types, with the highest variability occurring within the mixed  
14 LU type. The recreational LU type had the smallest increase in impervious surface but the largest  
15 areal percentage of vegetation. However, the largest total area of increase in impervious surface  
16 and vegetation was generated by the residential LU type. Small areas of inland water developed  
in some LU types but were absent from the industrial and transportation categories.

**Table 3**

Percentage coverage and total area of the different anthropogenic LC types within each LU type for years 1990, 2001, 2011.

LU type	Impervious surface		Vegetation		Water	
	Percentage	Area (km <sup>2</sup> )	Percentage	Area (km <sup>2</sup> )	Percentage	Area (km <sup>2</sup> )
<b>1990</b>						
Industrial	14.7	25.7	0.0	0.0	0.0	0.0
Mixed	18.5	34.3	1.5	2.9	0.0	0.0
Residential	12.0	45.6	2.9	10.9	0.0	0.0
Transportation	13.8	12.4	0.0	0.0	0.0	0.0
Recreational	1.0	0.3	3.9	1.1	0.0	0.0
<b>2001</b>						
Industrial	27.2	47.5	0.2	0.3	0.0	0.0
Mixed	35.5	66.1	2.8	5.3	0.0	0.0
Residential	25.0	95.2	3.2	12.2	0.0	0.0
Transportation	29.3	26.4	0.0	0.0	0.0	0.0
Recreational	2.3	0.7	20.9	5.9	0.2	0.1
<b>2011</b>						
Industrial	65.3	114.2	0.2	0.4	0.0	0.0
Mixed	74.7	139.0	3.2	5.9	0.8	1.5
Residential	60.4	229.5	5.5	21.0	0.1	0.3
Transportation	63.6	57.2	0.1	0.1	0.0	0.0
Recreational	5.8	1.6	46.2	12.9	0.7	0.2

Note. These are overall values based on all of the urban zones for each LU type. Number of zones of each LU type in each year are: industrial (10), mixed (11), residential (15), transportation (5) and recreational (14).

1

#### 2 **4.2 Spatial and temporal variability of LST and albedo**

3

4

5

6

7

8

9

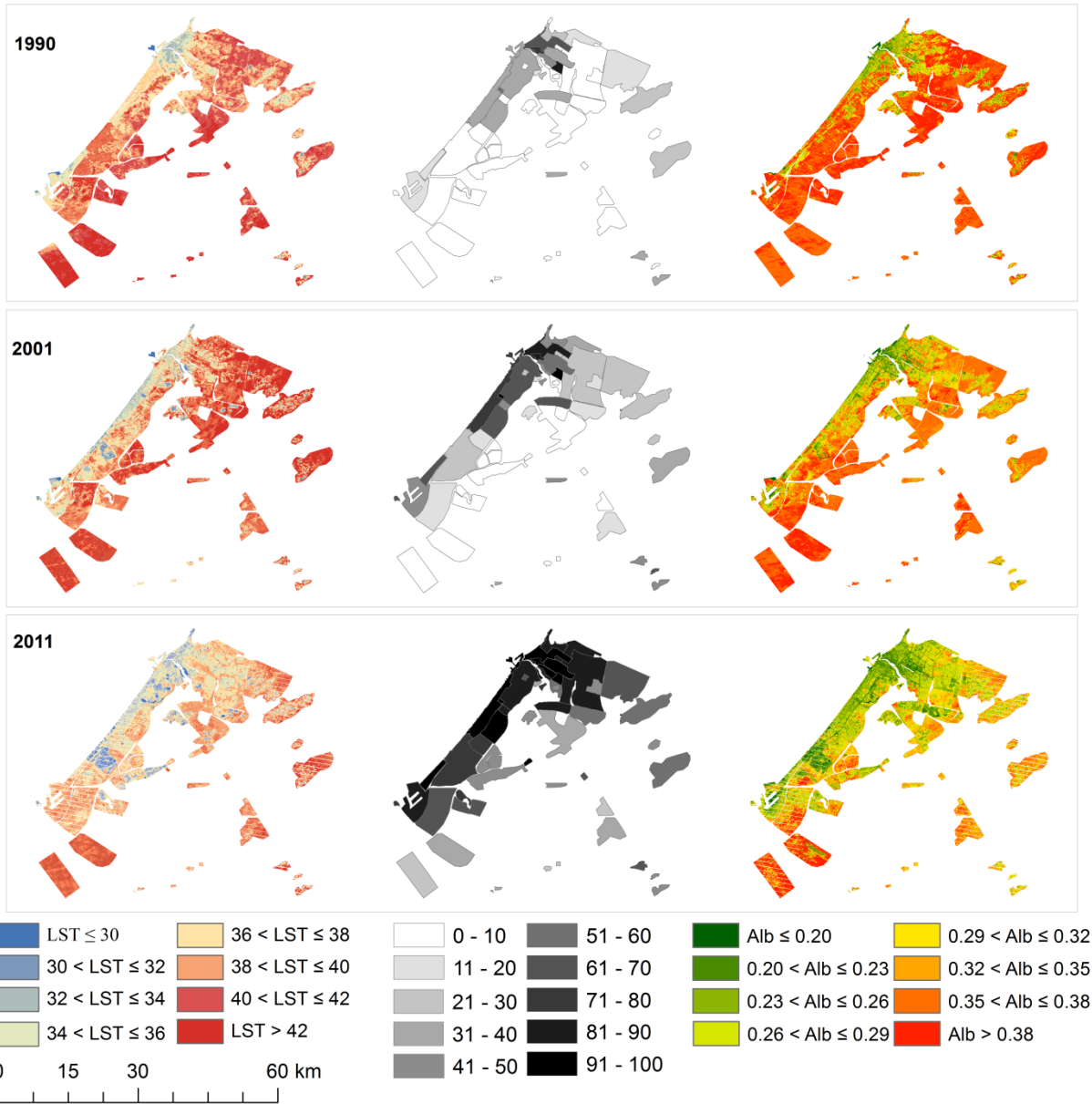
10

11

12

Figure 5 shows the spatial variations over time in LST, the percentage of anthropogenic land cover (combined impervious surface, vegetation and water) and albedo in each urban zone for the extent of the area that became urban by the end of the study period (UA<sub>2011</sub>). For the UA<sub>2011</sub>, average LST was highest in 1990 (42.28 °C), slightly lower in 2001 (41.71 °C) and lower still in 2011 (41.10 °C). The average LST relative to the desert sample areas (LST<sub>r</sub>) of the UA<sub>2011</sub> in 1990 was -0.28 °C (Standard Deviation (SD)= 0.49 °C). This average cooling effect increased to -0.74 °C in 2001 (SD= 0.93 °C) and was greater still in 2011 (-1.56 °C; SD= 1.3 °C). These data demonstrate how the development of the urban area has generated an overall cooling effect and that urban surface temperatures have become more variable. Such findings concerning

- 1 daytime LST are consistent with the results of other studies in desert cities (Frey et al., 2007) but
- 2 here we are demonstrating how the UHS has developed as the city has grown.



3

**Figure 5.** For the extent of the urban area in 2011 ( $UA_{2011}$ ) these images show the development over time in LST in  $^{\circ}C$  (left column), percentage of anthropogenic land cover (combined impervious surface, vegetation and water) in each urban zone (middle column) and albedo (right column).

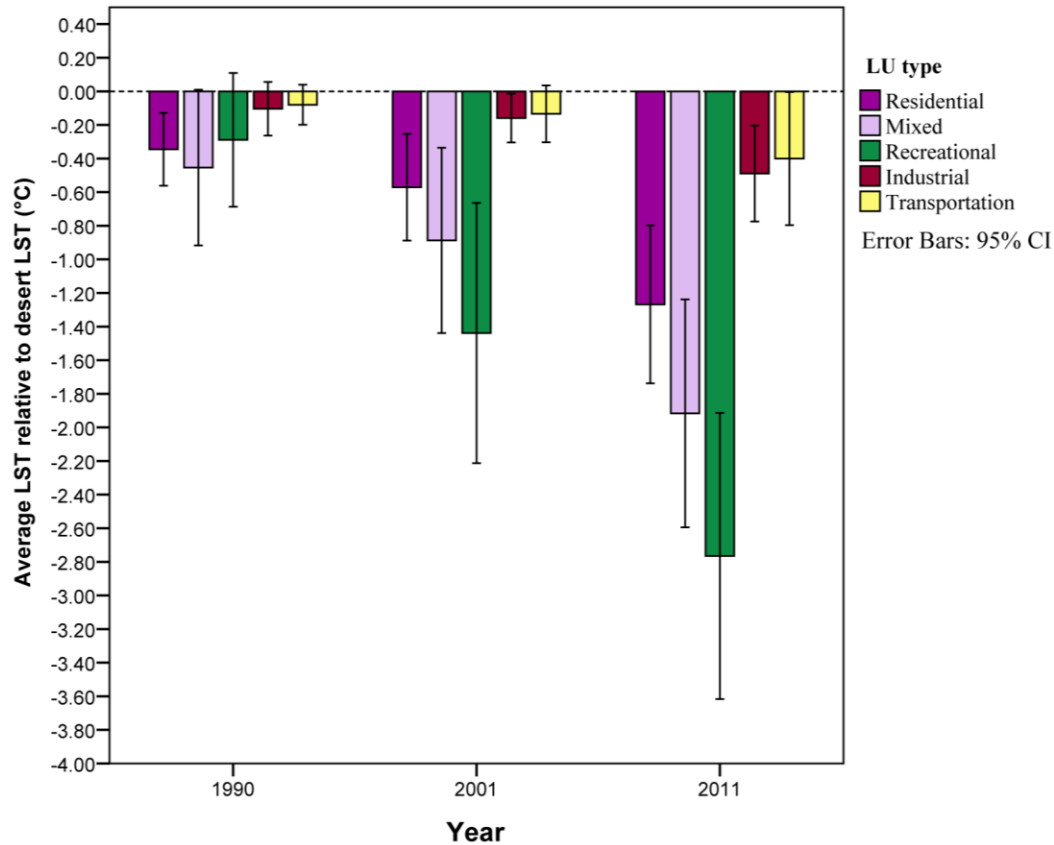
- 4 Visual interpretation of the map of LST (Figure 5) suggests an increase in the extent of
- 5 surface cooling throughout the study period and a decline in the extent of surfaces with high

1 temperatures. By comparing this to the map of percentage of anthropogenic LC, it can be seen  
2 that the areas of highest LST occur over undeveloped natural sands. In contrast, the coolest areas  
3 are concentrated in zones with high proportions of anthropogenic LC. Specifically, areas of low  
4 LST are noticeable in the central urban zones around the Creek in all of the sample years and  
5 areas of low LST spread along the coastal strip where anthropogenic LC increases through 2001  
6 and 2011.

7 Figure 5 also shows the changes over time in the spatial distribution of albedo. Average  
8 albedo for the UA<sub>2011</sub> was highest in 1990 (0.307), decreased in 2001 (0.297) and was lower still  
9 in 2011 (0.279). The average albedo of the UA<sub>2011</sub> was lower than the desert sample areas, with a  
10 difference of -0.014 (*SD*= 0.032) in 1990. This difference increased to -0.040 (*SD*= 0.041) in  
11 2001 and -0.064 (*SD*= 0.055) in 2011. This shows how the process of urbanization has converted  
12 the desert sand surface which has a high and more homogenous albedo into anthropogenic  
13 surfaces which have lower albedo with greater spatial heterogeneity. Figure 5 also shows that  
14 that albedo has a similar pattern to that of LST and that the highest LST and albedo values occur  
15 in zones with the lowest proportion of anthropogenic LC. Similar trends in LST and albedo have  
16 been previously noted in desert cities (Frey et al., 2007). So despite the decrease in albedo  
17 between 1990 and 2011 for the UA<sub>2011</sub> of Dubai, LST still decreases and, indeed, there is a high  
18 positive correlation between albedo and LST ( $r= 0.651$ ; based on data from the 55 urban zones).  
19 As we would normally expect a negative correlation between albedo and LST, with low  
20 reflectance surfaces absorbing more solar radiation and therefore experiencing higher  
21 temperatures, it would appear that factors other than albedo must be responsible for the decrease  
22 in LST as the urban area of Dubai has developed.

### 1 *4.3 Temporal variability of LSTr for the different LU types*

2           Figure 6 shows the magnitude of the difference in LST between each of the LU types and  
3 the desert (i.e.  $LST_d$ ) for each of the three sample years. This demonstrates that all of the urban  
4 LU types experienced lower temperatures than the desert on all occasions and that the cooling  
5 effect increased over time, but the magnitude of the change varied considerably between LU  
6 types. The increase in the cooling effect can be attributed to the increase in the area of the zones  
7 converted to urban LU as the city expanded between 1990 and 2011. In 1990 the largest cooling  
8 effect was experienced in the mixed LU type, followed by residential, recreational, industrial and  
9 transportation. By 2001 the cooling effect was most pronounced in the recreational LU type, then  
10 the mixed, residential, industrial and transportation types. A similar ranking was observed in  
11 2011. The error bars in Figure 6 demonstrate that there is an increase in the variability of the  
12 cooling effect for all LU types over time, implying an increase in the spatial heterogeneity of the  
13 UHS within and between different LU types as the city developed.



1

**Figure 6.** Average LST relative to desert ( $LST_r$ ) for the different LU types, with 95% confidence intervals (CI). In this figure the LU type refers to the LU which dominates the urban zones by the end of the study period (2011) and does not necessarily reflect the LU type that dominated in previous years (1990 and 2001) when most zones were dominated by sand.

2 **4.4 Relationships between  $LST_r$  and LC**

3

4

The relationships between  $LST_r$  and the three different types of land cover were examined to determine how the proportions of impervious surface, vegetation and water contribute to the UHS effect in Dubai. The analysis was based on a combined data set of  $LST_r$  and LC percentages for all of the urban zones for all of the sample years. Stepwise multiple regression analysis (see Draper and Smith, 1998) was used to select the LC types (as independent variables) according to their statistical contribution in explaining the variance in  $LST_r$  (as the dependent variable). Initially the independent variables were tested for multicollinearity and the

10

1 variance inflation factor and tolerance value (Brace et al., 2009) indicated a lack of correlation.  
 2 This indicated that all of the independent variables (%impervious, %vegetation and %water)  
 3 could be entered into a stepwise regression against  $LST_r$ , applying a 95% confidence interval  
 4 threshold for variable selection. The two models derived from stepwise regression (Table 4)  
 5 demonstrate that %vegetation and %impervious surface contributed significantly to explaining  
 6 the variance in  $LST_r$ , such that as these cover types increased, the cooling effect increased.  
 7 %vegetation accounted for 32% of the variance in  $LST_r$  while %impervious surface explained a  
 8 further 11% of the variance. However, %water had no relationship with  $LST_r$  in either of the two  
 9 models.

**Table 4**

Results of stepwise regressions between  $LST_r$  and the areal percentage of LC types, derived from data from all of the urban zones across all three sample years.

Contributor	Model 1		Model 2	
	<i>B</i>	95% CI	<i>B</i>	95% CI
Constant	-.571**	[-.725, -.416]	-.168	[-.371, -.036]
%vegetation	-3.238**	[- 3.996, - 2.510]	-3.743**	[-4.438, -3.048]
%impervious			-1.192**	[-1.622, -.762]
%water				
$R^2$	.321		.427	
<i>F</i>	77.122**		60.391**	
$R^2$ change			.106	
<i>F</i> change			29.958	

Note.  $N= 165$ , *B*= unstandardized coefficients, CI = confidence interval, \*\*=  $p < .01$ ,  $R^2$ =proportion variance explained; *F*= F statistic.

10

#### 11 ***4.5 Relationships between $LST_r$ and LC within the different LU types***

12

13 In order to understand the impacts of LC change on  $LST_r$  within each LU type in Dubai, a  
 14 set of stepwise multiple regression analyses were performed. These regressions were based on  
 15 separate data sets of  $LST_r$  and LC percentages derived from all of the zones of each LU type

1 across all three of the sample years. All independent variables (%impervious, %vegetation and  
 2 %water) for each LU type were tested and found not to exhibit multicollinearity. The stepwise  
 3 regressions produced a single statistically significant model for each of the LU types (Table 5).  
 4 These models demonstrated that  $LST_r$  was relatively well explained by %impervious surface in  
 5 four LU types (industrial, transportation, residential and mixed), whereby an increase in %  
 6 impervious surface generates an increased cooling effect, but %vegetation and %water make no  
 7 contribution. There was a wide variation between LU types in the variance in  $LST_r$  that was  
 8 explained by %impervious surface, ranging from a maximum of 85% in the mixed LU type to  
 9 63% in the industrial. This suggests that while the areal percentage of impervious surface is a  
 10 dominant control on the magnitude of the cooling effect, other factors such as the thermal  
 11 properties of the impervious materials used or the geometry of the urban environment (dealt with  
 12 in the next section) may also be influential. In the recreational LU type,  $LST_r$  was well explained  
 13 by the increase in %vegetation, accounting for 72% of the variance, while %impervious surface  
 14 and %water made no contribution.

**Table 5**

Results of stepwise regressions between  $LST_r$  and the areal percentage of LC types, for each LU type.

LU type	Industrial	Transportation	Recreational	Residential	Mixed
Model# <i>B</i>	1	1	1	1	1
Constant	.016	.127	-.572*	-.131	-.155
%Vegetation			-4.253**		
%impervious	-.627**	-.716**		-2.941**	-3.656**
%Water					
$R^2$	.627	.769	.721	.763	.852
$F$	18.059**	54.894 **	42.520**	43.052**	82.282**
$R^2$ change					
$F$ change					
$N$	30	15	42	45	33

Note. \*\*= $p < .01$ , \*= $p < .05$ .

1 **4.6 Relationships between LST and urban geometry**

2 Figure 7 uses a sample area of central Dubai to demonstrate how LST varies in response  
3 to the distribution of buildings. To quantify this effect, data from the 116 communities were used  
4 to examine the relationships between LST (for the year 2011) and each of the four urban  
5 geometry variables (average building height, building height variation, building density and  
6 %shading). Bivariate linear regression revealed that LST had a significant negative relationship  
7 with all variables (Table 6). The weakest correlation was between LST and building height  
8 variation, with stronger relationships for building density and average building height. The  
9 highest correlation was between LST and %shade. The results of the shadow analysis suggest  
10 that 17km<sup>2</sup> of the land surface was shaded by buildings at the time of 2011 Landsat image  
11 acquisition (4.3% of the total urban area). Figure 8 shows that the shade cast by buildings varies  
12 considerably depending upon building height and density and comparison with Figure 7  
13 illustrates how variations in shading influence the detected LST.

**Table 6**  
Correlation between LST and urban geometry variables.

Variable	Average building height	Building height variation	Building density	%Shade
LST	-.561	-.237	-.426	-.592

Note. N= 116, all correlations are significant at the 0.01 level (2-tailed).

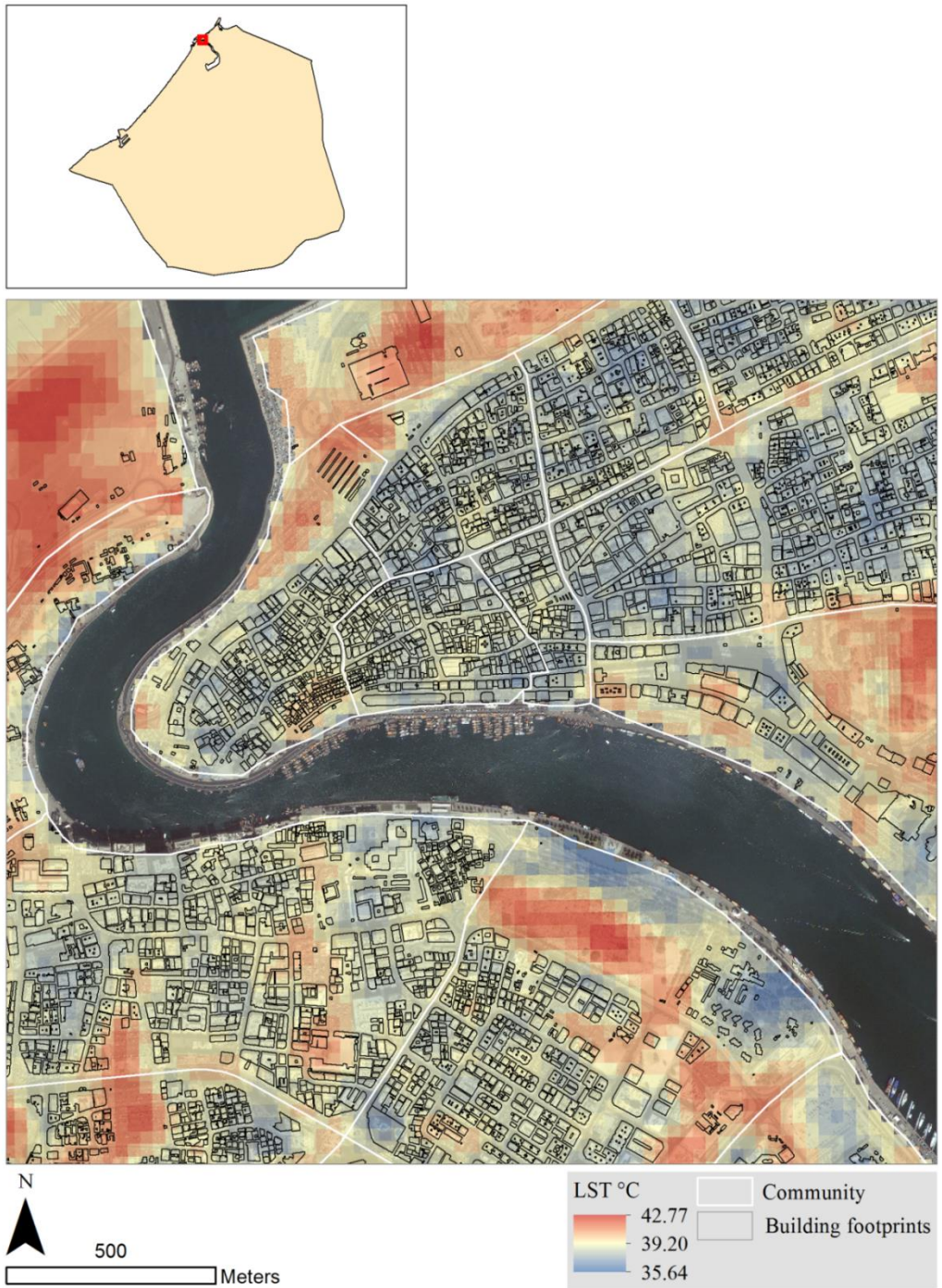


**Figure 7.** Sample area from central Dubai city demonstrating the correspondence between LST (from 2011 Landsat data) and building distribution, demonstrating the cooling effect of dense urban areas. The white lines show the boundaries of the community areas which were used as sampling units for analyzing relationships between urban geometry variables and LST. The red square on the inset map of Dubai emirate shows the position of the sample area used in the main map.

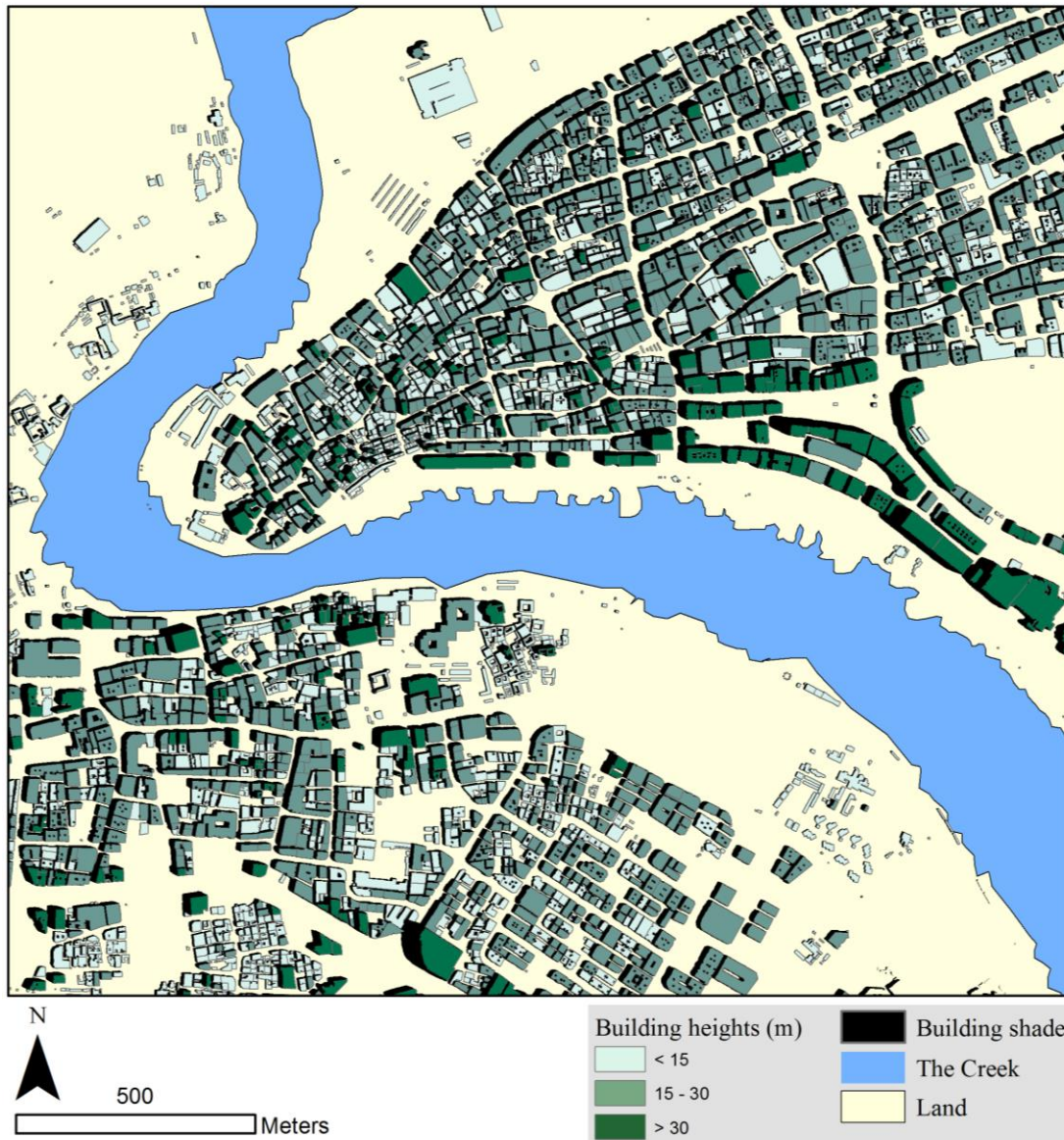


**Figure 8.** Sample area from central Dubai city (same area as Figure 7) showing the shade cast by buildings and variation in building heights.

1 **5. Discussion**

2  
 3           The transition of the desert environment to anthropogenic LC types has resulted in  
 4 substantial changes in LST in Dubai. Since 1990, the desert sands have been transformed into  
 5 impervious surfaces, vegetation and inland water as a consequence of population increase,  
 6 economic prosperity and government policy (see Nassar et al., 2014 for detailed discussion of

1 these issues). By comparing LC across the urban area of Dubai in 2011 with the same area in  
2 1990 we have demonstrated that impervious surface cover has increased from 14 to 64%,  
3 vegetation from 1.5 to 4.7% and water bodies from 0 to 0.2%. This increase in anthropogenic  
4 land cover has occurred at the expense of desert sand which is the main natural land cover across  
5 the emirate. This is quite different to other desert cities in the region such as Muscat in Oman  
6 (Al-Awadhi, 2007) and Doha in Qatar (Al-Manni et al, 2007) which have experienced a decrease  
7 in vegetation cover with increased urbanization.

8         In this study the LST of natural desert areas was set as a benchmark to provide a  
9 comparison for the LST of the anthropogenic LC types that have been introduced via  
10 urbanization in Dubai. The desert consistently had the highest LST during the 21-year study  
11 period and there has been a systematic decrease in the LST of urban zones that were under  
12 development (between 1990-2001 and 2001-2011). The zones that were fully developed in 1990  
13 or 2011 showed only a small variation in LST by the following sample date. These findings have  
14 allowed us to quantify the development of the UHS during a rapid phase of urban growth. It is  
15 worth noting that previous work has demonstrated that diurnally the maximum UHS effect  
16 occurs at the time of maximum temperature during the afternoon (Carnahan and Larson, 1990)  
17 therefore our measurements from Landsat images acquired during the morning are likely to  
18 underestimate the magnitude of the UHS. Our findings provide valuable evidence of the spatial  
19 variations in the UHS within the city and the temporal variations in response to urban growth. It  
20 should be noted that values of LST have been found to be higher than air temperatures at the  
21 same location, though with similar temporal trends (Coutts and Harris, 2012; Yuan and Bauer,  
22 2007), meaning that air temperatures experienced by the residents of Dubai are likely to be lower  
23 than the LST values reported here.

1           Our statistical analysis (Table 4) revealed that vegetation cover percentage explained  
2 32% of the variance in the cooling effect during the study period. Vegetation increases latent  
3 heat loss through the evapotranspiration which in turn generates a temperature decrease on and  
4 above the vegetated surface (e.g. Voogt and Oke, 2003). This cooling effect of urban vegetation  
5 is consistent with previous studies of other cities in desert environments (e.g. Lazzarini et al.,  
6 2013). However, water bodies made no significant contribution to cooling in Dubai which is  
7 probably explained by the very small amount of water in any of the urban zones.

8           The increase in the percentage of impervious surface over the study period has also  
9 contributed to the UHS, accounting for 11% of the variance in the cooling effect. It is feasible  
10 that the daytime cooling effect of impervious surfaces such as buildings, pavements and roads  
11 might be due to differences in specific heat capacity between construction materials and  
12 surrounding desert sands. Indeed, it is the case that published values of specific heat capacity for  
13 typical construction materials such as asphalt, aluminum, concrete and bricks (920, 897, 880 and  
14 840 J/kgK) are higher than that for sand (835 J/kgK) (Physics Hypertextbook, 2014). This would  
15 indicate that for a given input of energy the temperature of desert sand would show a larger  
16 increase in temperature than the impervious urban surfaces. It has to be noted that the observed  
17 rate of increase in LST in response to solar radiation input may also be influenced by other  
18 factors such as surface reflectivity, thermal conductivity and surrounding materials or objects.  
19 Nevertheless, it would appear that the higher specific heat capacity of urban materials may have  
20 some contribution to the UHS in desert cities and this is worthy of further investigation.  
21 However, the present study has demonstrated that the magnitude of the UHS effect in Dubai is  
22 significantly influenced by urban geometry. In particular, LST was negatively correlated with  
23 average building height and percentage of shade (Table 6) because taller buildings provide

1 greater shadow which reduces the amount of solar energy reaching the land surface (e.g. Kato et  
2 al., 2010).

3 The combined influence of heat capacity of urban materials and urban geometry on the  
4 UHS effect has been recognized in other cities (Erell and Williamson, 2007; Yang et al, 2016),  
5 yet the relative contribution of these factors has been more difficult to assess. In this study, the  
6 relative contribution of the heat capacity and urban geometry towards the UHS in Dubai can be  
7 assessed when we investigate the temporal changes in anthropogenic LC and the magnitude of  
8 the cooling effect in the individual LU types. Figure 9 shows that all the different urban LU types  
9 have experienced some cooling throughout the study period and the cooling effect has increased  
10 as the percentage of anthropogenic LC has increased. This figure also demonstrates visually how  
11 LU types containing vegetation have a proportionally larger cooling effect than those LU types  
12 that contain only impervious surfaces. Nevertheless those LU types with only impervious  
13 surfaces (industrial and transport) do show the cooling effect and this increases as the percentage  
14 cover of impervious surface increases through the study period. Because vegetation is present in  
15 much smaller amounts than impervious surfaces in most LU types, our statistical analysis (Table  
16 5) shows that the dominant influence on cooling in industrial, transportation, residential and  
17 mixed LU types is the amount of impervious surface cover. Such findings concur with those of  
18 Frey et al. (2007) who found that in desert cities even industrial urban areas with no vegetation  
19 and water coverage had lower LST than the surrounding desert environment. This is the case for  
20 both transportation and industrial LU types in Dubai where both have negligible vegetation  
21 coverage (<0.23%) and low buildings heights, so shading is minimal, yet they still show a  
22 cooling effect. Therefore, it is likely that the UHS in these LU types is attributable to the thermal  
23 properties of impervious surface materials such as specific heat capacity. As similar materials are

1 used in all of the LU types then their contribution to the UHS effect is likely to be ubiquitous.  
2 However, the UHS is considerably enhanced in the residential and mixed LU types due to  
3 shading by taller buildings.

4

5

6

7

8

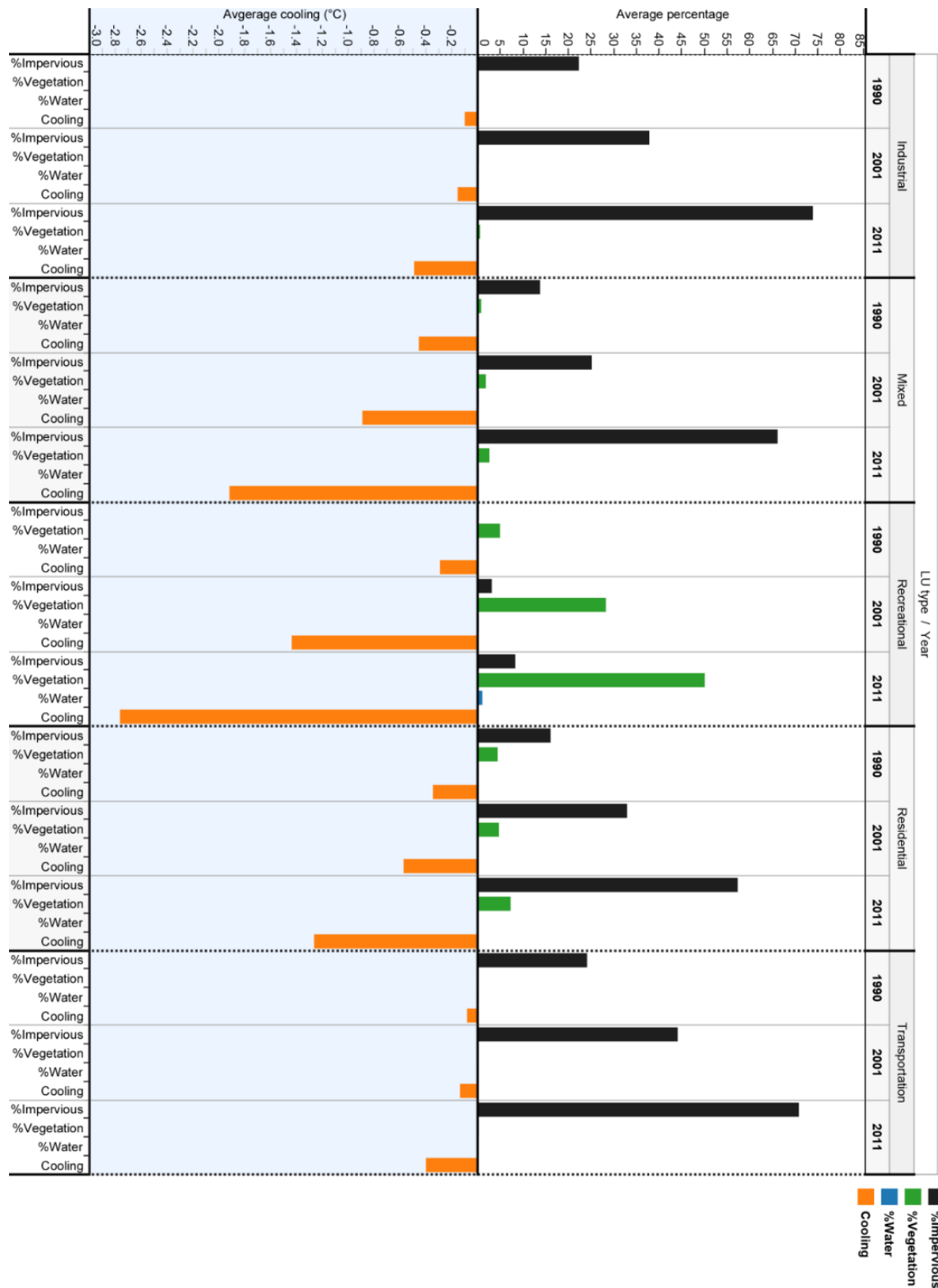


**Figure 9.** Changes over time (1990, 2001 and 2011) in the percentage of anthropogenic land covers (impervious surface, vegetation and water) within each land use type and the magnitude of the associated surface cooling effect (LST<sub>r</sub>). The figure is best viewed in landscape orientation.

1           The findings of this study call for some consideration of what aspects of the urban  
2 surface energy balance are actually being measured from a satellite's perspective. This issue has  
3 previously been recognized by Voogt and Oke (2003). In the present study, the shading analysis  
4 raises questions about the measurement of albedo, the physical property of a surface which  
5 describes the fraction of total incoming light that it reflects. In this study, and many others,  
6 Landsat waveband reflectance is used to estimate albedo, but surface reflectance is calculated  
7 assuming the same amount of incoming radiation across the whole scene. For ground areas that  
8 are shaded by buildings this assumption is invalid, so we must be underestimating reflectance  
9 and therefore underestimating albedo. Indeed, Frey and Parlow (2009) used radiation modelling  
10 to show that shading in dense urban areas can reduce estimates of albedo by up to 50% when the  
11 solar incidence angle was low in winter. So from a satellite perspective, we are not estimating the  
12 albedo of all areas of the land surface in the urban area, but deriving an estimate of the overall  
13 albedo of the wider urban area which Frey and Parlow (2009) term a nadir-view 'regional'  
14 albedo. This may explain why our measurements of albedo from Landsat show a decrease in  
15 albedo with urbanization, in that the decrease is likely responding to the increase in shading in  
16 urban areas in addition to the decrease in the albedo of the actual urban surfaces relative to the  
17 highly reflective desert sands. This, in turn, may provide a rationale for our observation that LST  
18 decreases despite albedo also decreasing with urban development.

19           Given the above discussion it is also important to consider the measurements of urban  
20 LST derived from Landsat, which are probably best described as nadir-view 'regional' surface  
21 temperature. The 'regional' term explains that observations are made of both illuminated and  
22 shaded surfaces, while 'nadir view' notes that the thermal imagery does not detect radiation  
23 being directly emitted from the vertical sides of buildings, which may vary between the extremes

1 of being directly illuminated with higher surface temperatures and in shade with lower  
2 temperatures. Therefore it could be argued that this is a limitation of using thermal imagery from  
3 satellites to understand surface temperatures in urban environments, as not all surfaces are being  
4 measured. As building heights increase, the proportion of vertical surfaces that are not imaged  
5 from nadir will increase and this may introduce inconsistencies when comparing surface  
6 temperature measurements across low-rise and high-rise urban areas. In their study of complete  
7 urban surface temperatures Voogt and Oke (1997) commented on the proportions of 'seen' and  
8 'unseen' surfaces noting that (vertical) walls made up 28% of active surfaces in light industrial  
9 areas (with horizontal surfaces, including rooftops, making up the remaining 72%) but 54% in  
10 downtown areas containing high-rise buildings. The nadir-view 'regional' surface temperature  
11 provided by Landsat and similar systems does offer the great benefit of being able to cover a  
12 wide area and it would be very difficult to obtain temperature measurements of an entire city by  
13 other means. Nevertheless, the issues raised here suggest that further research is needed to fully  
14 understand the advantages and limitations of satellite-based measurements of urban surface  
15 temperature and albedo.

16         The discussion of the remote sensing methodology and radiation interactions within  
17 urban structures provides some basis for considering the possible mechanisms that generate the  
18 observed UHS. The explanation could be partly due to differences in heat capacity, as discussed  
19 above, where urban materials require more energy input to raise their surface temperature.  
20 However, urban geometry is also likely to be influential. During most of the daytime, solar  
21 radiation will be impinging on the illuminated sides of buildings at a lower incidence angle than  
22 it will when reaching largely horizontal desert surfaces. So the same amount of energy will be  
23 distributed across a larger surface area on the sides of the buildings, thereby reducing surface

1 temperatures. In addition, the three dimensional urban environment has a larger total surface area  
2 than the planar desert surface and while both receive the same solar input, the urban environment  
3 has greater capacity to emit thermal radiation and thus reduce surface temperatures, effectively  
4 acting like a heat sink on a computer processor. So the greater emissions combined with the  
5 effects of the low incidence angles on illuminated building sides, the areas of shadow this creates  
6 and higher specific heat capacity of urban materials may produce the heat sink effect relative to  
7 the desert observed in the Landsat thermal imagery. Clearly, the validity of this mechanism and  
8 the relative contribution of the different processes are worthy of further investigation.

## 9 **6. Conclusions**

10  
11 This study has demonstrated how the development of the desert city of Dubai has  
12 generated an overall cooling effect. All types of urban LU generated a lower LST than the desert  
13 and there was an increase in the spatial heterogeneity of the UHS within and between different  
14 LU types as the city developed. This study has presented useful evidence concerning the relative  
15 influence of vegetation and impervious surfaces on the UHS in desert cities, which has been  
16 subject to some uncertainty (Frey et al., 2007, Imhoff et al., 2010; Lazzarini et al., 2013). Where  
17 urban vegetation was planted LST reduced substantially and the amount of vegetation cover is an  
18 important influence on the UHS, but impervious surfaces dominate the urban area of Dubai and  
19 are responsible for the majority of the heat sink effect. Albedo, as measured from Landsat, is  
20 positively correlated with LST and therefore appears to not be causally related to the UHS effect.  
21 However, it was found that urban geometry was related to the magnitude of cooling of LST,  
22 particularly through the effects of shadows cast by buildings. The urban geometry has  
23 implications for the remote sensing of urban albedo and LST which warrant further investigation  
24 and future research on the effects of LC transitions and type of LU on LST within desert cities

1 will be valuable. In particular, a deeper understanding of the interactions between the thermal  
2 properties of construction materials, urban vegetation and urban geometry is now needed. This  
3 has potential to inform future urban designs which promote the thermal comfort of residents and  
4 minimize energy demands for active cooling of built infrastructure and transport systems in  
5 desert cities.

1 **Acknowledgements**

2

3 The authors would like to express their gratitude to the U.S. Geological Survey and Dubai  
4 governmental departments for providing the data. Helpful comments from anonymous reviewers  
5 are acknowledged.

## References

- Al-Awadhi, T. (2007). Monitoring and modeling urban expansion using GIS & RS: Case study from Muscat, Oman. *Urban Remote Sensing Joint Event, IEEE*. doi: 10.1109/URS.2007.371790.
- Al-Manni, A. A., Abdu, A. S., Mohammed, N. A., & Al-Sheeb, A. E. (2007). Urban growth and land use change detection using remote sensing and geographic information system techniques in Doha City, State of Qatar. *Arab Gulf Journal for Scientific Research*, 25(4), 190-198.
- Anderson, J. M., Hardy, E. E., Roach, J. T., & Witmer, R. E. (1976). *A land use classification system for use with remote sensing Data*. Geological Survey Professional Paper. Washington D. C.: Government Printing Office.
- Brace, N., Kemp, R., & Snelgar, R. (2009). *SPSS for Psychologists: A Guide To Data Analysis* (4<sup>th</sup> ed.). Basingstoke: Palgrave Macmillan Limited.
- Bretz, S., Akbari, H., & Rosenfeld, A. (1998). Practical issues for using solar-reflective materials to mitigate urban heat islands. *Atmospheric Environment*, 32, 95-101. [http://dx.doi.org/10.1016/S1352-2310\(97\)00182-9](http://dx.doi.org/10.1016/S1352-2310(97)00182-9).
- Carnahan, W.H., & Larson, R.C. (1990). An Analysis of an Urban Heat Sink. *Remote Sensing of Environment*, 33, 65-71. [http://dx.doi.org/10.1016/0034-4257\(90\)90056-R](http://dx.doi.org/10.1016/0034-4257(90)90056-R).
- Coseo, P., & Larsen, L. (2014). How factors of land use/land cover, building configuration, and adjacent heat sources and sinks explain Urban Heat Islands in Chicago. *Landscape and Urban Planning*, 125, 117–129. doi: 10.1016/j.landurbplan.2014.02.019
- Coutts, A., & Harris, R., 2012. Urban Heat Island Report: A multi-scale assessment of urban heating in Melbourne during an extreme heat event: policy approaches for adaptation. Victorian Centre for Climate Change Adaptation Research.
- Draper, N.R., & Smith, H. (1998). *Applied Regression Analysis* (3rd ed., pp.335-339). New York: John Wiley & Sons, Inc.
- Dubai Airport (2014). *Climate*. <https://services.dubaiairports.ae/DubaiMet/Met/Climate.aspx>. Retrieved 15.5.14.
- Dubai Statistical Centre (2011). *Population Bulletin: Emirates of Dubai*. <http://www.dsc.gov.ae/EN/Themes/Pages/Publications.aspx?TopicId=23>. Retrieved 21.05.12.
- Erell, E., Pearlmutter, D., & Williamson, T. (2011). *Urban Microclimate: designing the spaces between buildings* (1st ed.) London: EarthScan.
- Erell, E., & Williamson, T.(2007). Intra-urban differences in canopy layer air temperature at a mid-latitude city. *International Journal of Climatology*, 27(9), 1243–1255. doi: 10.1002/joc.1469
- Frey, C. M. & Parlow, E. (2009). Geometry effect on the estimation of band reflectance in an urban area. *Theoretical and Applied Climatology*, 96, 395-406.
- Frey, C. M., Rigo, G., & Parlow, E. (2007). Urban radiation balance of two coastal cities in a hot and dry environment, *International Journal of Remote Sensing*, 28(12), 2695 2712. <http://dx.doi.org/10.1080/01431160600993389>.
- Hamdi, R., & Schayes, G. (2009). Sensitivity study of the urban heat island intensity to urban characteristics. *The seventh International Conference on Urban Climate, 29 June - 3 July*. Yokohama, Japan.
- Hu, L., & Brunsell, N.A. (2013). The impact of temporal aggregation of land surface temperature data for surface urban heat island (SUHI) monitoring. *Remote Sensing of Environment*, 134, 162–174. <http://dx.doi.org/10.1016/j.rse.2013.02.022>.
- Imhoff, M.L., Zhang, P., Wolfe, R.E., & Bounoua, L. (2010). Remote sensing of the urban heat island effect across biomes in the continental USA. *Remote Sensing of Environment*, 114, 504–513. <http://dx.doi.org/10.1016/j.rse.2009.10.008>.
- Jensen, J. R. (2005). *Introductory digital image processing a remote sensing perspective* (3<sup>rd</sup> ed.). USA: Prentice Hall Series in geographic information science.

- Johansson, E., & Emmanuel, R. (2006). The influence of urban design on outdoor thermal comfort in the Hot Humid City of Colombo, Sri Lanka. *International Journal of Biometeorology*, *51*, 119-133. doi: 10.1007/s00484-006-0047-6.
- Kato, S., Matsunaga, T., & Yamaguchi, Y. (2010). Influence of shade on surface temperature in an urban estimated by ASTER data. *International Archives of the Photogrammetry, Remote Sensing and Spatial Information Science*, *38*, 925-929.
- Kayadibi, O. (2011). Evaluation of imaging spectroscopy and atmospheric correction of multispectral images (Aster and Landsat 7 ETM+). *Proceedings, 5th Int. Conf. Recent Advances in Space Technologies (RAST), 9-11 June.*, Istanbul. pp. 154-159. doi: 10.1109/RAST.2011.5966811.
- Lazzarini, M., Marpu, P.R., & Ghedira, H. (2013). Temperature-land cover interactions: The inversion of urban heat island phenomenon in desert city areas. *Remote Sensing of Environment*, *130*, 136-152. <http://dx.doi.org/10.1016/j.rse.2012.11.007>.
- Liang, S. (2000). Narrowband to broadband conversions of land surface albedo I Algorithms. *Remote Sensing of Environment*, *76*, 213- 238.
- Littlefair, P.J., Santamouris, M., Alvarez, S., Dupagne, A., Hall, D., Teller, J., et al. (2000). *Environmental site layout planning: solar access, microclimate and passive cooling in urban areas* (1<sup>st</sup> ed.). Watford: CRC.
- Lo, C. P., & Choi, J. (2004). A hybrid approach to urban land use/cover mapping using Landsat 7 Enhanced Thematic Mapper Plus (ETM+) images. *International Journal of Remote Sensing*, *25(14)*, 2687-2700. <http://dx.doi.org/10.1080/01431160310001618428>.
- Mackey, C.W., Lee, X., & Smith, R.B. (2012). Remotely sensing the cooling effects of city scale efforts to reduce urban heat island. *Building and Environment*, *49*, 348-358. <http://dx.doi.org/10.1016/j.buildenv.2011.08.004>.
- Martin, J., Kurc, S.A., Zaines, G., Crimmins, M., Hutmacher, A., & Green, D. (2012). Elevated air temperatures in riparian ecosystems along ephemeral streams: The role of housing density. *Journal of Arid Environments*, *84*, 9-18. <http://dx.doi.org/10.1016/j.jaridenv.2012.03.019>.
- Nassar, A.K., Blackburn, G.A., & Whyatt, J.D. (2014). Developing the desert: The pace and process of urban growth in Dubai. *Computers, Environment and Urban Systems*, *45*, 50-62. <http://dx.doi.org/10.1016/j.compenvurb.2014.02.005>.
- National Bureau of Statistics (2010). UAE Population by Emirates, Nationality and Sex. <http://www.uaestatistics.gov.ae/ReportDetailsEnglish/tabid/121/Default.aspx?ItemId=1869&PTID=104&MenuId=1>. Retrieved 21.03.12.
- Omran, E.E. (2012). Detection of land-use and surface temperature change at different resolutions. *Journal of Geographic Information System*, *4*, 189-203. <http://dx.doi.org/10.4236/jgis.2012.43024>.
- Physics Hypertextbook (2014). <http://physics.info/heat-sensible/>. Retrieved 01.02.2014.
- Skyscraper Center. (2014). <http://www.skyscrapercenter.com>. Retrieved 02.01.14.
- Snyder, W.C., Wan, Z., Zhang, Y., & Feng, Y.Z. (1998). Classification-based emissivity for land surface temperature measurement from space. *International Journal of Remote Sensing*, *19(14)*, 2753-2774. doi:10.1080/014311698214497
- US EPA (2008). *Reducing urban heat islands: Compendium of strategies*. United States Environmental Protection Agency, Washington, D.C. <http://www.epa.gov/hiri/resources/compendium.htm>. Retrieved 12.11.13.
- Verbyla, D. L., & Hammond, T. O. (1995). Conservative bias in classification accuracy assessment due to pixel-by-pixel comparison of classified images with reference grids. *International Journal of Remote Sensing*, *16*, 581-587. <http://dx.doi.org/10.1080/01431169508954424>.
- Voogt, J.R., & Oke, T.R. (1997). Complete Urban Surface Temperatures. *Journal of Applied Meteorology*, *36*, 1117-1132.
- Voogt, J.R., & Oke, T.R. (2003). Thermal remote sensing of urban climates. *Remote Sensing of Environment*, *86(3)*, 370-384. [http://dx.doi.org/10.1016/S0034-4257\(03\)00079-8](http://dx.doi.org/10.1016/S0034-4257(03)00079-8).

- Weng, Q. (2001). A remote sensing-GIS evaluation of urban expansion and its impact on surface temperature in the Zhujiang Delta, China. *International Journal of Remote Sensing*, 22, 1999–2014. doi: 10.1080/713860788.
- Wu, C., Lung, S.C., Jan, F. (2013). Development of a 3-D urbanization index using digital terrain models for surface urban heat island effects. *ISPRS Journal of Photogrammetry and Remote Sensing*, 81, 1–11. <http://dx.doi.org/10.1016/j.isprsjprs.2013.03.009>
- Yang, X., Li, Y., Luo, Z., & Chan, P. W. (2016), The urban cool island phenomenon in a high-rise high-density city and its mechanisms. *Int. J. Climatol.* doi:10.1002/joc.4747
- Yuan, F., & Bauer, M.E. (2007). Comparison of impervious surface area and normalized difference vegetation index as indicators of surface urban heat island effects in Landsat imagery. *Remote Sensing of Environment*, 106, 375–386. <http://dx.doi.org/10.1016/j.rse.2006.09.003>
- Zhang, H., Qi, Z.-f., Ye, X.-y., Cai, Y.-b., Ma, W.-c., & Chen, M.-n (2013). Analysis of land use/land cover change, population shift, and their effects on spatiotemporal patterns of urban heat islands in metropolitan Shanghai, China. *Applied Geography*, 44, 121-133. doi:10.1016/j.apgeog.2013.07.021